demonstrated devices with Seebeck coefficients as high as 12 μV/K (at $T = 40$ K) and high electronic temperature $\Delta T \sim 4.5$ K (*14*). Hot carrier–assisted photoresponse is predicted to improve the power conversion efficiency of energy-harvesting devices beyond standard limits (*29*). Our findings, together with new design principles for next-generation solar thermoelectric devices (*30*), make graphene-based systems viable for energy-harvesting applications.

References and Notes

1. S. M. Sze, *Physics of Semiconductor Devices* (Wiley, London, ed. 2, 1981).
2. V. Sukhovatkin, S. Hinds, L. Brzozowski, E. H. Sargent, *Science* **324**, 1542 (2009).
3. N. M. Gabor, Z. Zhong, K. Bosnick, J. Park, P. L. McEuen, *Science* **325**, 1367 (2009).
4. R. Bistritzer, A. H. MacDonald, *Phys. Rev. Lett.* **102**, 206410 (2009).
5. T. Winzer, A. Knorr, E. Malic, *Nano Lett.* **10**, 4839 (2010).
6. J. C. Song, M. S. Rudner, C. M. Marcus, L. S. Levitov, *Nano Lett.* 10.1021/nl202318u (2011).
7. E. J. Lee, K. Balasubramanian, R. T. Weitz, M. Burghard, K. Kern, *Nat. Nanotechnol.* **3**, 486 (2008).
8. J. Park, Y. H. Ahn, C. Ruiz-Vargas, *Nano Lett.* **9**, 1742 (2009).
9. F. Xia, T. Mueller, Y. M. Lin, A. Valdes-Garcia, P. Avouris, *Nat. Nanotechnol.* **4**, 839 (2009).
10. T. Mueller, F. Xia, P. Avouris, *Nat. Photonics* **4**, 297 (2010).
11. G. Nazin, Y. Zhang, L. Zhang, E. Sutter, P. Sutter, *Nat. Phys.* **6**, 870 (2010).
12. X. Xu, N. M. Gabor, J. S. Alden, A. M. van der Zande, P. L. McEuen, *Nano Lett.* **10**, 562 (2010).
13. M. C. Lemme *et al.*, *Nano Lett.* 10.1021/nl2019068 (2011).
14. See supporting material on *Science* Online.
15. B. Huard *et al.*, *Phys. Rev. Lett.* **98**, 236803 (2007).
16. J. R. Williams, L. Dicarlo, C. M. Marcus, *Science* **317**, 638 (2007).
17. B. Özyilmaz *et al.*, *Phys. Rev. Lett.* **99**, 166804 (2007).
18. E. H. Hwang, E. Rossi, S. Das Sarma, *Phys. Rev. B* **80**, 235415 (2009).
19. P. Wei, W. Bao, Y. Pu, C. N. Lau, J. Shi, *Phys. Rev. Lett.* **102**, 166808 (2009).
20. Y. M. Zuev, W. Chang, P. Kim, *Phys. Rev. Lett.* **102**, 096807 (2009).
21. J. Checkelsky, N. P. Ong. *Phys. Rev. B* **80**, 081412(R) (2009).
22. D. Sun *et al.*, *Phys. Rev. Lett.* **101**, 157402 (2008).
23. J. H. Strait *et al.*, *Nano Lett.* 10.1021/nl202800h (2011).
24. N. W. Ashcroft, N. D. Mermin, *Solid State Physics* (Thomson Learning Inc., London, 1976).
25. In the top-gated region, both V_{BG} and V_{TG} contribute to n_c, resulting in the slope of the diagonal line $m = \Delta V_{TG}/\Delta V_{BG} = C_{BG}/C_{TG} \approx 0.05$, where C_{BG} and C_{TG} are respectively the bottom- and top-gate capacitances to graphene. $\mathbf{N}_B$ and $\mathbf{N}_T$ in the Fourier transform are perpendicular to the minimum resistance lines (gray dashed lines) in Fig. 2A.
26. E. McCann, *Phys. Rev. B* **74**, 161403 (2006).
27. T. Ohta, A. Bostwick, T. Seyller, K. Horn, E. Rotenberg, *Science* **313**, 951 (2006).
28. E. V. Castro *et al.*, *Phys. Rev. Lett.* **99**, 216802 (2007).
29. R. T. Ross, A. J. Nozik, *J. Appl. Phys.* **53**, 3813 (1982).
30. D. Kraemer *et al.*, *Nat. Mater.* **10**, 532 (2011).

Acknowledgments: We thank M. Baldo, P. McEuen, P. Kim, and A. Yacoby for valuable discussions. Supported by the Air Force Office of Scientific Research, a NSF Early Career Award (P.J.H.), and the Packard Foundation. Sample fabrication was performed at the NSF-funded MIT Center for Materials Science and Engineering and Harvard Center for Nanoscale Science.

Supporting Online Material

www.sciencemag.org/cgi/content/full/science.1211384/DC1
Materials and Methods
SOM Text
Figs. S1 to S4
References (*31*–*38*)

19 July 2011; accepted 26 September 2011
Published online 6 October 2011;
10.1126/science.1211384

The Pace of Shifting Climate in Marine and Terrestrial Ecosystems

Michael T. Burrows,[1]* David S. Schoeman,[2,3] Lauren B. Buckley,[4] Pippa Moore,[5,6] Elvira S. Poloczanska,[7] Keith M. Brander,[8] Chris Brown,[7,9] John F. Bruno,[4] Carlos M. Duarte,[10,11] Benjamin S. Halpern,[12] Johnna Holding,[11] Carrie V. Kappel,[12] Wolfgang Kiessling,[13] Mary I. O'Connor,[14] John M. Pandolfi,[15] Camille Parmesan,[16] Franklin B. Schwing,[17] William J. Sydeman,[18] Anthony J. Richardson[7,9,19]

Climate change challenges organisms to adapt or move to track changes in environments in space and time. We used two measures of thermal shifts from analyses of global temperatures over the past 50 years to describe the pace of climate change that species should track: the velocity of climate change (geographic shifts of isotherms over time) and the shift in seasonal timing of temperatures. Both measures are higher in the ocean than on land at some latitudes, despite slower ocean warming. These indices give a complex mosaic of predicted range shifts and phenology changes that deviate from simple poleward migration and earlier springs or later falls. They also emphasize potential conservation concerns, because areas of high marine biodiversity often have greater velocities of climate change and seasonal shifts.

Climate warming is a global threat to biodiversity (*1*). Key mechanisms allowing species to cope with warming include shifting biogeographic ranges and altering phenology (the synchronous timing of ecological events) (*2*, *3*) to accommodate spatial and seasonal changes in ambient temperature. Considerable variation in species responses exists: Average range shifts have been reported as 6.1 km/decade for terrestrial communities (*2*), from 1.4 to 28 km/decade for marine communities (*4*), and 16.1 km/decade for a combination of both (*5*), whereas spring phenology has been reported as advancing on average by 2.3 to 2.8 days/decade on land (*2*, *6*) and by 4.3 days/decade at sea (*3*, *7*). One reason for variability in estimates of responses could be that patterns of climate change are dynamic and highly heterogeneous across Earth. Different regions are warming or even cooling at different rates, and air temperatures are rising faster than those of upper ocean waters (*8*), so uniform responses across the globe to climate change should not be anticipated. Instead, organism responses are expected to track the rate of isotherm migration over space and seasons to maintain their thermal niches (*9*, *10*).

Although organisms may respond to aspects of climate change other than temperature, our aim was to generate predictions for shifts in distribution and phenology from physical descriptions of the global thermal environment, and to compare predictions among regions across the land and ocean. We used global surface temperatures (*11*, *12*) over 50 years (1960–2009) to calculate the distribution of the velocity and seasonal shifts of isotherm migration over land and ocean on a 1°-by-1° grid (*7*). The velocity of climate change (*10*) (in km/year) was calculated as the ratio of the long-term temperature trend (in °C/year)

[1]Department of Ecology, Scottish Association for Marine Science, Scottish Marine Institute, Oban, Argyll, PA37 1QA, Scotland, UK. [2]Environmental Sciences Research Institute, School of Environmental Sciences, University of Ulster, Coleraine, BT52 1SA, Northern Ireland. [3]Department of Zoology, Post Office Box 77000, Nelson Mandela Metropolitan University, Port Elizabeth, 6031, South Africa. [4]Department of Biology, University of North Carolina at Chapel Hill, Chapel Hill, NC 27599, USA. [5]Institute of Biological, Environmental and Rural Sciences, Aberystwyth University, Aberystwyth, SY23 3DA, UK. [6]Centre for Marine Ecosystems Research, Edith Cowan University, Perth, 6027, Australia. [7]Climate Adaptation Flagship, Commonwealth Scientific and Industrial Research Organisation Marine and Atmospheric Research, Ecosciences Precinct, General Post Office Box 2583, Brisbane, Queensland 4001, Australia. [8]National Institute of Aquatic Resources, Technical University of Denmark, Charlottenlund Slot, Jægersborg Allé 1, Charlottenlund, Denmark. [9]School of Biological Sciences, University of Queensland, Brisbane, Queensland 4072, Australia. [10]The University of Western Australia Oceans Institute, University of Western Australia, 35 Stirling Highway, Crawley 6009, Australia. [11]Department of Global Change Research, Instituto Mediterráneo de Estudios Avanzados (Consejo Superior de Investigaciones Científicas, University of the Balearic Islands), Esporles, 07190, Spain. [12]National Center for Ecological Analysis and Synthesis, University of California Santa Barbara, 735 State Street, Suite 300, Santa Barbara, CA 93101, USA. [13]Museum für Naturkunde at Humboldt University, Invalidenstrasse 43, 10115 Berlin, Germany. [14]Department of Zoology and Biodiversity Research Centre, University of British Columbia, Vancouver, Canada V6T 1Z4. [15]School of Biological Sciences, Australian Research Council Centre of Excellence for Coral Reef Studies, University of Queensland, Brisbane, Queensland 4072, Australia. [16]Section of Integrative Biology, 1 University Station C0930, University of Texas, Austin, TX 78712, USA. [17]Southwest Fisheries Science Center, National Oceanic and Atmospheric Administration Fisheries Service, 1352 Lighthouse Avenue, Pacific Grove, CA 93950, USA. [18]Farallon Institute for Advanced Ecosystem Research, Post Office Box 750756, Petaluma, CA 94975, USA. [19]Centre for Applications in Natural Resource Mathematics, School of Mathematics and Physics, University of Queensland, St Lucia, Queensland 4072, Australia.

*To whom correspondence should be addressed. E-mail: michael.burrows@sams.ac.uk

to the two-dimensional spatial gradient in temperature (in °C/km, calculated over a 3°-by-3° grid), oriented along the spatial gradient. We introduced the seasonal climate shift (in days/decade) as the ratio of the long-term temperature trend (°C/year) to the seasonal rate of change in temperature (°C/day). We present seasonal shifts for spring and fall globally using April and October temperatures.

The median rate of warming since 1960 has been more than three times faster on land (0.24°C/decade) than at sea (0.07°C/decade, Fig. 1A and table S1). At the scale of our analysis, median spatial gradients in temperature on land (0.0082°C/km, Fig. 1B and table S1) are greater than those at sea (0.0030°C/km) because of the greater latitudinal and topographical temperature differences on land, whereas large-scale currents tend to reduce small-scale variability in ocean surface temperatures. When spatial gradients are combined with rates of long-term temperature change, the resulting median velocity of isotherms across the ocean (21.7 km/decade) is 79% of that on land (27.3 km/decade), but when comparing only those latitudes where both land and ocean are present (50°S to 80°N), velocities in the ocean (27.5 km/decade) are similar to those on land (27.4 km/decade). The frequency distribution of velocities in the ocean is bimodal (Fig. 2A), with a broader spread of positive values in the ocean than on land and many negative values in cooling areas, including the Southern Ocean and Eastern Boundary Current regions with increased upwelling (Fig. 1, A and C, and fig. S1D). The relative proportions of warming and cooling areas influence the land/ocean comparison (table S1): With less cooling, median velocity in the Northern Hemisphere ocean is 37.3 km/decade but only 30.3 km/decade on land, whereas in the Southern Hemisphere median velocities are 17.6 and 14.6 km/decade for land and ocean, respectively. The velocity of climate change is two to seven times faster in the ocean than on land in the sub-Arctic and within 15° of the equator (Fig. 1C), but ocean and land velocities are similar at most other latitudes (20° to 50°S and 15° to 45°N).

At the scales studied, the velocity of climate change is very patchy on land, whereas the ocean

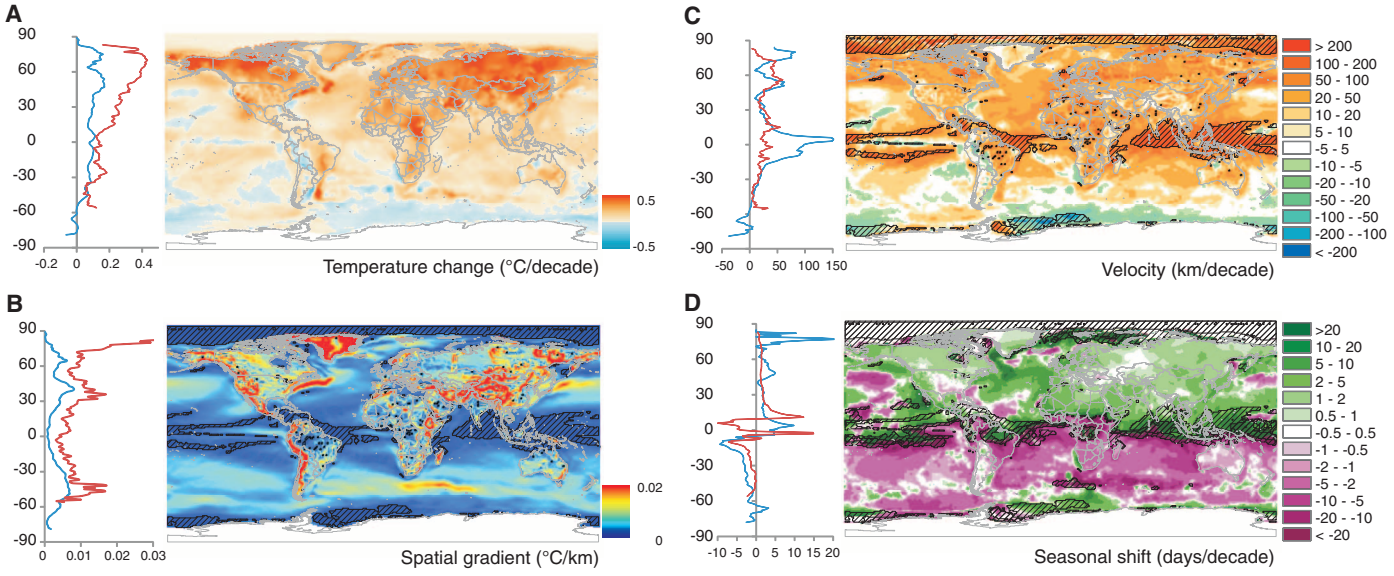

Fig. 1. (**A**) Trends in land (Climate Research Unit data set CRU TS3.1) and ocean (Hadley Centre data set Had1SST 1.1) temperatures for 1960–2009, with latitude medians (red, land; blue, ocean). (**B**) Spatial gradients in annual average temperatures using the same data; cross-hatching shows areas with shallow spatial gradients (<0.1°C/degree). (**C**) The velocity of climate change (km/decade) is the velocity at which isotherms move: positive in warming areas, negative in cooling areas, and generally faster in areas of shallow spatial gradients. (**D**) Seasonal shift (days/decade) is the change in timing of monthly temperatures, shown for April, representing Northern Hemisphere spring and Southern Hemisphere fall: positive where timing advances, negative where timing is delayed. Cross-hatching shows areas with small seasonal temperature change (<0.2°C/month), where seasonal shifts may be large. See fig. S3 for October seasonal shifts.

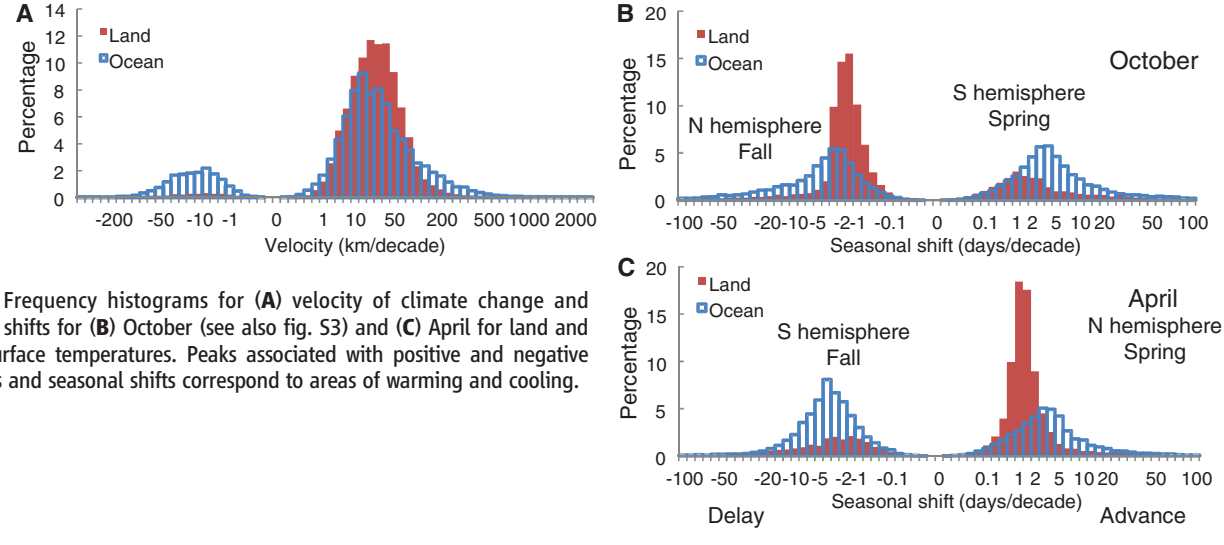

Fig. 2. Frequency histograms for (**A**) velocity of climate change and seasonal shifts for (**B**) October (see also fig. S3) and (**C**) April for land and ocean surface temperatures. Peaks associated with positive and negative velocities and seasonal shifts correspond to areas of warming and cooling.

surface has homogenous surface temperatures with shallow spatial gradients separated by relatively sharp thermal boundaries (Fig. 1, B and C). Areas of high velocity therefore extend across broader regions in the ocean than on land, and this may help explain the 1.5 to 5 times faster average range shifts reported in the ocean (*4*, *13*) than on land (*2*, *4*), albeit from few taxa in mainly temperate regions (*2*–*4*, *6*) in areas where the velocities of climate change are similar across land and ocean. Geographical variation in the velocity of climate change may explain much of the variation among range shifts of individual species (*5*), and shifts relative to our predictions may indicate sensitivity to temperature. This may explain some of the differences in reported averages from marine and terrestrial meta-analyses.

Despite faster warming on land, change in seasonal timing is generally greater in the ocean because of smaller seasonal thermal variation (fig. S2, A to C). Shifts in the timing of spring temperatures (1960–2009) were 30 to 40% faster in the ocean than on land (table S1). Spring ocean temperatures arrived earlier by 2.08 days/decade in the Northern Hemisphere and 2.52 days/decade in the Southern Hemisphere (median values excluding equatorial regions), but by 1.46 and 2.15 days/decade, respectively, on land. Equatorial regions were excluded from these estimates because small seasonal temperature change gave high values for shifts (fig. S2, B and C) and because the lack of strong annual variation (fig. S2A) suggests that temperature is not a driver of tropical phenology. A greater advance in spring timing in the ocean than on land was evident in the Arctic (>66°N, Fig. 1D) and in mid-latitudes (40° to 60°N). Considerable variability exists in the Southern Ocean, with delayed springs in cooling areas and advanced springs in warming areas (fig. S3).

Delays in the arrival of colder fall temperatures were also greater in the ocean than on land in both hemispheres (medians for the northern ocean were 1.73 days/decade and for land 1.20 days/decade; for the southern ocean, 2.28 days/decade and for land 1.21 days/decade, table S1). The land/ocean difference was consistent across most latitudes in the Southern Hemisphere (Fig. 1D) but was only greater in the ocean in the Northern Hemisphere beyond 45°N (fig. S3). Large areas of land have negligible seasonal change, particularly in central Asia. Later springs in central North America are associated with a spring cooling trend. Estimates of spring seasonal shift are close to reported global average values for earlier timing of boreal spring events [2.3 days/decade (*2*), 5.1 days/decade (*14*), and 2.8 days/decade (*6*)]. Rates of spring advance exceed this in the North Atlantic and North Pacific, the Arctic Ocean, and much of Europe, North America, and eastern Asia (Fig. 1D).

Our indices of change relate to almost all terrestrial species but only to those marine species that live at or near the surface. Many marine species, however, depend on surface conditions, using light for energy or plants for food or having surface-living planktonic stages. For terrestrial species, the option exists to move to greater altitude to track thermal conditions, but depth changes have been reported for only a few marine organisms, such as fish (*15*–*17*) and hydroids (*18*). For species that cannot adjust their depth, range shifts may be limited by the availability of suitable habitat. Where such habitat is not aligned with the velocity of climate change, as happens on east-west coastlines (*19*), the velocity along the axis of the habitat could be much faster (*7*).

Considerable geographical heterogeneity exists in rates of velocity of climate change and magnitude of seasonal shift, with consequences for life on land (*10*) and in the ocean that depend on biophysical attributes of regions (Fig. 3, fig. S4, and table S2). Land/ocean boundaries constrain movement, as in the Mediterranean, where species may be forced toward the European continent, away from potential escape routes (Fig. 3C and table S2). Adjacent areas of rapid poleward and equatorward velocities exist, as seen near the Antarctic Peninsula (Fig. 3E), and spring conditions can be both advanced and delayed within small regions (Fig. 3, B and D). Thus, subregional and habitat-specific patterns in temperature may run counter to the simple expectation of poleward range shift and shifts toward earlier spring and later fall, and biological responses will vary accordingly (*20*).

Accumulated negative effects of high velocities (*21*) and rapid seasonal shifts on many species may threaten biodiversity, especially where such conditions coincide with species-rich equatorial and coastal regions (*22*, *23*), as in the Coral Triangle (Fig. 3A and table S2). For example, in tropical areas where spatial gradients are shallow, the rapid velocity of climate change may be of special concern: No communities of organisms from even warmer regions exist to replace those moving out (*24*). Likewise, as polar areas warm, resident organisms might lose their current thermal niches altogether. In contrast, areas of low

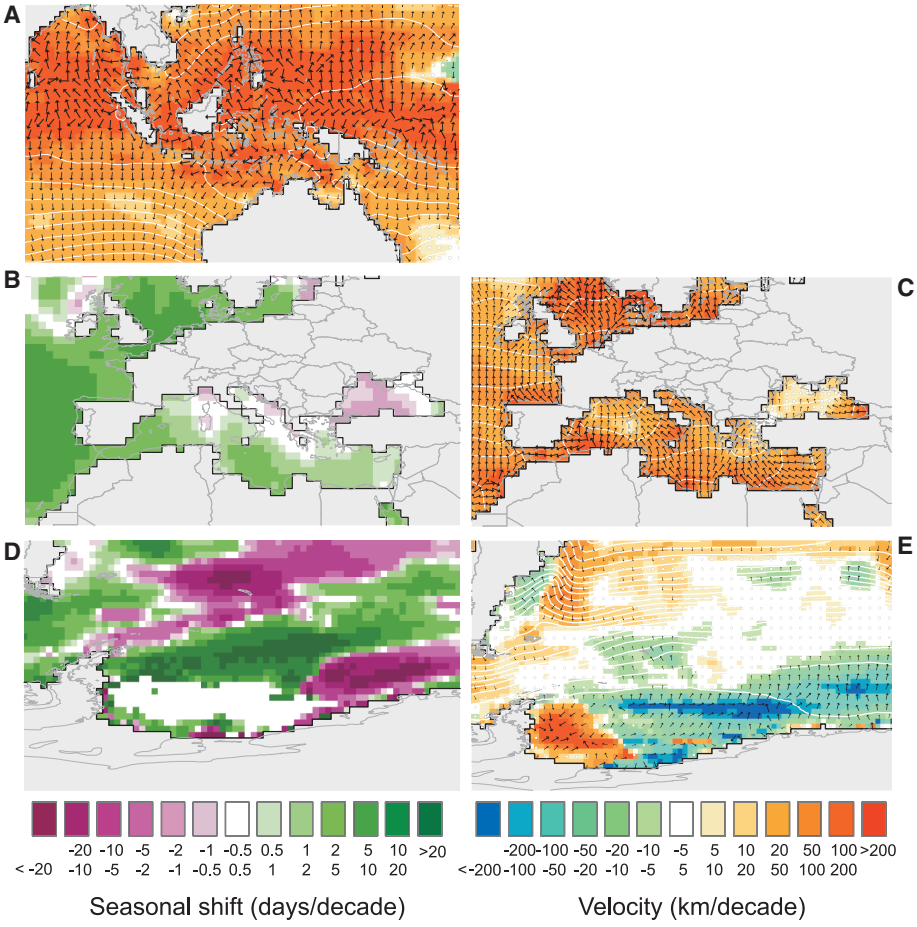

Fig. 3. Within-region patterns of seasonal shifts and velocity of climate change in the ocean. Arrows illustrate the magnitude and direction of velocity, perpendicular to isotherms (white lines); circles indicate velocities <1 km/decade. (**A**) Rapid divergent velocities in the Coral Triangle. (**B**) Spring temperatures arrived 5 to 10 days/decade earlier in the North Sea but by less in the Mediterranean and were delayed in the Black Sea. (**C**) Poleward velocities in the Mediterranean are constrained by the European landmass. (**D**) Spring temperatures arrived 10 to 20 days/decade earlier to the east of the Antarctic Peninsula but were delayed by a similar amount in adjacent areas of cooling. (**E**) Poleward velocities exist alongside equatorward velocities in the same region, suggesting location-specific responses of species ranges.

velocity or slow seasonal shifts, where residence times of climate would be longest (*10*), may be important repositories for biodiversity.

The global distribution of the velocity and seasonal shift of climate change over the past 50 years can be used to generate predictions for comparison with observed biological changes. Despite slower ocean warming, the velocity of climate change and seasonal shift in the ocean are as high as on land and often deviate from simple expectations of poleward migration and earlier springs/later falls. Direct effects of climate warming are therefore likely to be as great in the oceans as on land at comparable latitudes and greater around the equator. Maps of the velocity of climate change and seasonal shift show the areas where the threat to biodiversity from organisms' need to rapidly track thermal conditions by shifting distributions and retiming seasonal thermal events may be greatest; these areas may coincide with high biodiversity, especially in the oceans.

References and Notes

1. O. E. Sala *et al.*, *Science* **287**, 1770 (2000).
2. C. Parmesan, G. Yohe, *Nature* **421**, 37 (2003).
3. S. J. Thackeray *et al.*, *Glob. Change Biol.* **16**, 3304 (2010).
4. W. W. L. Cheung *et al.*, *Fish Fish.* **10**, 235 (2009).
5. I.-C. Chen, J. K. Hill, R. Ohlemüller, D. B. Roy, C. D. Thomas, *Science* **333**, 1024 (2011).
6. C. Parmesan, *Glob. Change Biol.* **13**, 1860 (2007).
7. Full methods are presented in the supporting material on *Science* Online.
8. K. E. Trenberth *et al.*, in *Climate Change 2007: The Physical Science Basis. Contribution of Working Group I to the Fourth Assessment Report of the Intergovernmental Panel on Climate Change*, S. Solomon *et al.*, Eds. (Cambridge Univ. Press, Cambridge, 2007), pp. 235–336.
9. D. D. Ackerly *et al.*, *Divers. Distrib.* **16**, 476 (2010).
10. S. R. Loarie *et al.*, *Nature* **462**, 1052 (2009).
11. UK Meteorological Office Hadley Centre, Natural Environment Research Council's National Centre for Atmospheric Science (NCAS) (British Atmospheric Data Centre, 2010); http://badc.nerc.ac.uk/view/badc.nerc.ac.uk__ATOM__dataent_hadisst.
12. University of East Anglia Climate Research Unit, NCAS (British Atmospheric Data Centre, 2010); http://badc.nerc.ac.uk/view/badc.nerc.ac.uk__ATOM__dataent_1256223773328276.
13. C. J. B. Sorte, S. L. Williams, J. T. Carlton, *Glob. Ecol. Biogeogr.* **19**, 303 (2010).
14. T. L. Root *et al.*, *Nature* **421**, 57 (2003).
15. A. L. Perry, P. J. Low, J. R. Ellis, J. D. Reynolds, *Science* **308**, 1912 (2005).
16. N. K. Dulvy *et al.*, *J. Appl. Ecol.* **45**, 1029 (2008).
17. J. A. Nye, J. S. Link, J. A. Hare, W. J. Overholtz, *Mar. Ecol. Prog. Ser.* **393**, 111 (2009).
18. S. Puce, G. Bavestrello, C. G. Di Camillo, F. Boero, *Mar. Ecol. (Berlin)* **30**, 313 (2009).
19. N. Mieszkowska, S. J. Hawkins, M. T. Burrows, M. A. Kendall, *J. Mar. Biol. Assoc. U.K.* **87**, 537 (2007).
20. B. Helmuth *et al.*, *Ecol. Monogr.* **76**, 461 (2006).
21. H. M. Pereira *et al.*, *Science* **330**, 1496 (2010).
22. P. H. Williams, K. J. Gaston, C. J. Humphries, *Proc. R. Soc. London Ser. B* **264**, 141 (1997).
23. D. P. Tittensor *et al.*, *Nature* **466**, 1098 (2010).
24. R. K. Colwell, G. Brehm, C. L. Cardelús, A. C. Gilman, J. T. Longino, *Science* **322**, 258 (2008).

Acknowledgments: This work was conducted as a part of the Towards Understanding Marine Biological Impacts of Climate Change Working Group supported by the National Center for Ecological Analysis and Synthesis, a Center funded by NSF (grant no. EF-0553768); the University of California, Santa Barbara; and the State of California. M.T.B. thanks the UK Natural Environment Research Council Oceans 2025 program, J.P. thanks the Australian Research Council Centre of Excellence for Coral Reef Studies for additional support, and A.J.R. was supported by the Australian Research Council Discovery Grant DP0879365 and Future Fellowship Grant FT0991722. Data used in analyses are available from the University of East Anglia Climate Research Unit and the UK Meteorological Office Hadley Centre, with online access at the British Atmospheric Data Centre.

Supporting Online Material

www.sciencemag.org/cgi/content/full/334/6056/652/DC1
Materials and Methods
SOM Text
Figs. S1 to S5
Tables S1 and S2
References (*25*–*45*)

24 June 2011; accepted 20 September 2011
10.1126/science.1210288

Atmospheric Blocking and Atlantic Multidecadal Ocean Variability

Sirpa Häkkinen,[1]* Peter B. Rhines,[2] Denise L. Worthen[3]

Atmospheric blocking over the northern North Atlantic, which involves isolation of large regions of air from the westerly circulation for 5 days or more, influences fundamentally the ocean circulation and upper ocean properties by affecting wind patterns. Winters with clusters of more frequent blocking between Greenland and western Europe correspond to a warmer, more saline subpolar ocean. The correspondence between blocked westerly winds and warm ocean holds in recent decadal episodes (especially 1996 to 2010). It also describes much longer time scale Atlantic multidecadal ocean variability (AMV), including the extreme pre–greenhouse-gas northern warming of the 1930s to 1960s. The space-time structure of the wind forcing associated with a blocked regime leads to weaker ocean gyres and weaker heat exchange, both of which contribute to the warm phase of AMV.

The climate of the global oceans undergoes natural variability with many time scales, as well as greenhouse-induced change. We discuss the relation between periods of warm subpolar ocean and patterns of blocking in the atmospheric circulation above in the North Atlantic sector. Blocking occurs when the high-latitude jet stream develops large, nearly stationary meanders, essentially breaking Rossby waves with precursors upwind, over North America. These trap an air mass equatorward of an anticyclonic pressure ridge. We show here that clusters of frequent blocking over the subpolar North Atlantic coincide with warm and saline ocean in the 1960s, late 1970s, and early 2000s (*1*). Further back in time, a new reconstruction of surface atmospheric pressure field for the entire 20th century (*2*, *3*) encompasses the most dramatic climate event of the century: the pre–greenhouse-gas northern warming that began in the 1920s and lasted until the 1960s. Sea surface temperatures (SST) of the North Atlantic also show this widespread warming, whereas the South Atlantic Ocean is cooler than normal. This longer time scale variability is known as Atlantic Multidecadal Variability (AMV, or Atlantic Meridional Oscillation, AMO) (*4*, *5*). AMV has been linked to many multidecadal climate processes: Atlantic hurricanes, northeast Brazil and Sahel rainfall, North American and European summer climate (*5*–*7*). We show that warm ocean and frequent atmospheric blocking coincide over multidecadal AMV time scales. More than a local response to the atmosphere, invasions of warm ocean water northward from the subtropics, extending well below the surface, are involved (*1*, *8*).

Atmospheric blocking involves shifts in Atlantic storm tracks lasting several days. Blocking over Greenland is associated with the negative phase of the North Atlantic Oscillation (NAO) and a southward shift of the storm track (*9*) (fig. S1). The blocking also occurs further east over western Europe with an anticyclone over the northern subpolar gyre (fig. S2). Such blocking is accompanied by cold winter temperatures in western Europe, for example, winters in 2005/2006 (*10*), 1963, and 2009/2010 (*11*). The climatological maximum in winter blocking days is located over western Europe, with a secondary maximum over Greenland connected by a ridge of increased blocking (fig. S3), if blocking is defined by absolute geopotential height index [(*12*), which is an extension of (*13*, *14*)]. Thus, the east-west location of Atlantic blocking anticyclones varies, but in 61 of 110 cases investigated in (*9*), European blocks immediately precede Greenland blocks.

[1]National Aeronautics and Space Administration (NASA) Goddard Space Flight Center, Code 615, Greenbelt, MD 20771, USA. [2]University of Washington, Box 357940, Seattle, WA 98195, USA. [3]Wyle Information Systems/NASA Goddard Space Flight Center, Code 615, Greenbelt, MD 20771, USA.

*To whom correspondence should be addressed. E-mail: sirpa.hakkinen@nasa.gov

The Pace of Shifting Climate in Marine and Terrestrial Ecosystems

Michael T. Burrows, David S. Schoeman, Lauren B. Buckley, Pippa Moore, Elvira S. Poloczanska, Keith M. Brander, Chris Brown, John F. Bruno, Carlos M. Duarte, Benjamin S. Halpern, Johnna Holding, Carrie V. Kappel, Wolfgang Kiessling, Mary I. O'Connor, John M. Pandolfi, Camille Parmesan, Franklin B. Schwing, William J. Sydeman, and Anthony J. Richardson

Science, 334 (6056), • DOI: 10.1126/science.1210288